박 사 학 위 논 문

Studies on Definition of Novel Functional Roles of RPL27 Gene in Colorectal Cancer Progression

계 명 대 학 교 대 학 원

의 학 과

박 소 영

지도교수 이 윤 한

2 0 2 2 년 2 월

Studies on Definition of Novel Functional Roles of RPL27 Gene in Colorectal Cancer Progression 박 소 영 2022년 2월

Studies on Definition of Novel Functional Roles of RPL27 Gene in Colorectal Cancer Progression

지도교수 이 윤 한

이 논문을 박사학위 논문으로 제출함

2022년 2월

계 명 대 학 교 대 학 원

의학과 분자의학 전공

박 소 영

박소영의 박사학위 논문을 인준함

주 심 이 재 호

부 심 이 윤 한

부 심 김 신

부 심 서 지 혜

부 심 이 태 진

계 명 대 학 교 대 학 원

2 0 2 2 년 2 월

Table of Contents

List of Tables

List of Figures

1. Introduction

In 2020, colorectal cancer (CRC) had the second highest mortality rate worldwide and was the third most common cancer type among various carcinomas, accounting for 10.0% and 9.4% of all carcinomas, respectively (1). CRC causative factors include excessive red meat and processed meat consumption, excessive drinking, smoking, inflammatory bowel disease, obesity, diabetes, and a family history of CRC (2-8). In addition, several genetic factors are involved in the development of colorectal neoplasia, including activation of oncogenes and inactivation of tumor suppressor genes (9). In particular, mutation of the tumor suppressor gene is important for the transition from non-invasive to invasive disease (10). The treatment of CRC mainly involves surgery, radiation therapy, and chemotherapy (11). The optimal treatment strategy for CRC patients depends on many factors, including age, performance status, presence of comorbidities, and treatment settings (adjuvant, palliative, and neoadjuvant) (12). However, these treatments have side effects such as increased risk of gastrointestinal, hematologic, and cardiac toxicities in patients with CRC (13).

Ribosomes are important organelles in cells. Their functions include genetic information translation of mRNA into proteins and cellular metabolism regulation. Several previous studies demonstrated that ribosome biogenesis is related to cell proliferation and that ribosome biogenesis plays a role in tumorigenesis (14). Protein constituents, called ribosomal proteins (RPs), have different functions in every species. RPs mainly play an important role in the synthesis and function of ribosomes. Furthermore, RPs act as a scaffold to enhance the catalytic ability of rRNA to synthesize proteins. Some RPs also have important

additional ribosome functions, such as DNA repair, transcriptional regulation, and apoptosis (15). RPs have been linked to human congenital diseases and cancers. For example, RPS4 is associated with Turner's syndrome (16), and mutations in RPS19 have been found in patients with Diamond-Blackfan anemia (17). RPL23, a gene related to tumor metastasis, was shown to induce high invasiveness in lung cancer cell lines (18). Many RPs are overexpressed in CRC, including RPL27 (19), RPS3 (20), RPS19 (21), and RPL7a (22).

A previous study has confirmed that the function of RPL27 gene is associated with liver cancer cell growth (23), but few studies have been conducted on definition of the extra-ribosomal function of RPL27 in CRC. Therefore, in this study, the extra-ribosomal function of RPL27 in CRC was investigated.

2. Materials and Methods

2.1. Bioinformatics analysis:

The expression of RPL27 in CRC was determined using Gene Expression Profiling Interactive Analysis (GEPIA). The Cancer Genome Atlas (TCGA) database was used to analyze gene correlations.

2.2. Cell culture:

Human CRC cell lines, HCT116 and HT29 were purchased from the Korean Cell Line Bank (KCLB, Seoul, South Korea). Both cell lines were cultured in RPMI-1640 medium supplemented with 1% penicillin/streptomycin solution and 10% fetal bovine serum (FBS) (Welgene, Daegu, South Korea).

2.3. Small interfering RNA (siRNA) transfection:

Before siRNA transfection, the cells were plated at a density of 30%. After 24 h, cells were transfected with 15 nM of siRNAs for 5 h with Lipofectamine 2000 (Invitrogen, Carlsbad, CA, USA) and Opti-MEM (Thermo Scientific Fisher, Rockford, IL, USA). The negative control (NC) siRNA was designed as follows: 5′-ACGUGACACGUUCGGAGAA(UU)-3′ (sense) and 5′-UUCUCCGAACGUGUCACGU-3′ (antisense). Three variants of RPL27-specific siRNAs (RPL27-1siRNA, ID# s12205; RPL27-2siRNA, ID# 9273; and RPL27-3siRNA, ID# 9361) were purchased from Ambion

(Austin, TX, USA).

2.4. MTT assay:

Cell growth was assessed using the 3-(4,5-dimethylthiazol-2-yl)-2,5-diphenyltetrazolium bromide (MTT) reagent, according to the manufacturer's instructions (Duchefa Biochemie, Haarlem, Netherlands). HCT116 and HT29 cells (1×10^3 cells) were transfected with siRNAs as described above. After 96 h, the cells were treated with the MTT reagent for 1 h. The OD value was evaluated at a wavelength of 540 nm using an Asys IVM 340 microplate reader (Biochrom, Cambridge, UK).

2.5. Quantitative real-time polymerase chain reaction (qRT-PCR):

Changes in gene expression at the mRNA level were measured using qRT-PCR. Total RNA was isolated using an RNeasy Plus Mini Kit (QIAGEN, Hilden, Germany), and cDNA was synthesized using a cDNA Synthesis Kit (Takara Biotech, Kusatsu, Shiga, Japan), according to the manufacturer's instructions. cDNAs were amplified using a corresponding pair of primers, which were synthesized by Genotech (Daejeon, South Korea). The primer sequences for qRT-PCR are listed in Table 1. Relative mRNA expression was assessed using LightCycler 96 (Roche, Basel, Switzerland) and quantified using LightCycler 96 software version 1.1, in comparison with the Ct (threshold cycle) values of each target gene, as stated in the manufacturer's instructions. In addition, mRNA levels were normalized using GAPDH mRNA levels as the control.

2.6. Clonogenic assay:

Cells transfected with NCsiRNA or RPL27siRNA were seeded onto 6-well plates and incubated in RPMI-1640 medium until viable cells propagated to sizable colonies for quantification. The number of colonies was counted using a microscope.

2.7. Cell cycle and apoptosis assay:

For the cell cycle and apoptosis assay, cells were cultured in 100-mm petri dishes and harvested 72 h after siRNA transfection. To measure the percentage of cells in each cell cycle phase, cells were incubated in the dark with propidium iodide (PI) staining solution containing RNase A (BD Bioscience, San Diego, CA, USA). For apoptosis analysis, cells were stained with both Annexin V and PI using an FITC Annexin V Apoptosis Detection Kit I (BD Bioscience), according to the manufacturer's instructions. Cell cycle and cell death were analyzed using an FACS Canto II flow cytometer (BD Bioscience) and quantified using the FACSDiva software program.

2.8. *In vivo* assay:

HCT116 cells were transfected with NCsiRNA or RPL27-1siRNA for 24 h and harvested. The cells were then resuspended in RPMI-1640 medium mixed with Matrigel (Corning, Corning, NY, USA). In total, 1×10^6 cells were injected subcutaneously into the left and right flanks of 4-week-old male BALB/c nude mice (Orientbio, Seongnam, South Korea). Tumor size was monitored and measured at two- or three-day

intervals for 21 days using a Vernier caliper. The tumor weight of each mouse was evaluated at the end of the observation period. All animal experiments were conducted under the approval number KM-2021-03, according to the guidelines of the Keimyung University Institutional Animal Care and Use Committee.

2.9. RNA sequencing:

RNA sequencing was performed as previously described (24). The datasets generated and analyzed in this study are accessible in the GEO public database (accession number GSE78195).

2.10. Western blotting:

Cells were suspended in a lysis buffer 48 h after siRNA transfection. Equal amounts of total protein were fractionated using sodium dodecyl sulphate-polyacrylamide gel electrophoresis (SDS-PAGE) on a gel and transferred to a polyvinylidene difluoride (PVDF) membrane (Roche). The membranes were blocked with 5% milk/Tris-buffered saline plus Tween 20 (TBST) and incubated with primary antibodies against RPL27 (Invitrogen), PLK1 (Santa Cruz Biotechnology, Cruz, CA, USA), p-CDC25C (Cell Signaling Technology, Danvers, MA, USA), CDK1 (Santa Cruz Biotechnology), cyclin B1 (Santa Cruz Biotechnology), β-actin (Santa Cruz Biotechnology), Flag (Sigma Aldrich, Saint Louis, MO, USA), and CD133 (Cell Signaling Technology). Anti-mouse HPR (Jackson ImmunoResearch Lab, West Grove, PA, USA) and goat anti-rabbit IgG-HRP (Santa Cruz Biotechnology) were used as secondary antibodies. Immunoreactive bands were visualized using

FUSIOM SOLO S (Vilber Lourmat, Marne La Vallee, France).

2.11. Migration and invasion assays:

Migration and invasion assays were performed using a Transwell migration assay (#3422, Corning) and 24-well Matrigel invasion chambers (#354480, Corning), respectively. For these assays, siRNA-transfected cells were plated in 24-well plates at 5×10^4 cells per well and incubated for 24 h. Then, the cells were fixed and stained with 0.5% crystal violet. Images were captured at 100× magnification under a microscope.

2.12. Plasmid transfection and overexpression of RPL27:

HCT116 cells were transiently transfected with a pCMV6-entry vector (Empty-vector) or an RPL27-expressing vector (RPL27-vector) (OriGene, Rockville, MD, USA) using Lipofectamine 2000.

2.13. Sphere forming assay:

Cells (5×10^3) were suspended in serum-free DMEM/F-12 medium containing 2% B27 (Invitrogen), 4 ng/mL insulin (Invitrogen), 10 ng/mL basic fibroblast growth factor, and 20 ng/mL epidermal growth factor. The cells were then seeded onto 24-well ultra-low attachment plates (Corning). After plating the cells, the cells were transfected with NCsiRNA or RPL27siRNA using Lipofectamine RNAiMAX (Invitrogen). The number of spheres was counted in 8 days of siRNA transfection.

2.14. Magnetic cell sorting and flow cytometry:

HT29 cells were trypsinized and resuspended in phosphate-buffered saline (PBS) with Fcr Blocking Reagent (130-100-857, CD133 MicroBead Kit, Miltenyi Biotec, Auburn, CA, USA). CD133 microbeads were added and incubated for 15 min at 4 °C in the dark. After washing, the labeled cells were separated using an AutoMACS Pro (Miltenyi Biotec). Magnetic labeled cells (CD133+ cells) and unlabeled cells (CD133- cells) were resuspended in PBS with isotype control antibody, mouse IgG2b, APC (130-122-932, Miltenyi Biotec), or CD133/2 antibody anti-human, APC (130-113-746, Miltenyi Biotec). The cells were incubated for 30 min at 4 °C in the dark. After washing, the separated cells were used to evaluate the efficiency of magnetic separation via FACSCanto II flow cytometry (BD Bioscience).

2.15. Statistical analysis:

All statistical analyses were repeated at least three times, and performed using Student's *t*-test, except for the analysis of GEPIA and TCGA data. All results are presented as the mean ± standard error of mean (SEM). $*p < 0.05$, $**p < 0.01$, and *** $p < 0.001$ were considered statistically significant.

Table 1. List of Primer Sequences for qRT-PCR

Name		Sequences
RPL27	forward	TGGCTGGAATTGACCGCTAC
	reverse	CCTTGTGGGCATTAGGTGATTG
GAPDH	forward	ACATCAAGAAGGTGGTGAAG
	reverse	GGTGTCGCTGTTGAAGTC
PLK1	forward	CTCAACACGCCTCATCCTC
	reverse	GTGCTCGCTCATGTAATTGC
CD133	forward	AGTCGGAAACTGGCAGATAGC
	reverse	GGTAGTGTTGTACTGGGCCAAT
NANOG	forward	CGATCTCCTGACCTTGT
	reverse	CACGCCTGTAAATCCCA
CD44	forward	CTGCCGCTTTGCAGGTGTA
	reverse	CATTGTGGGCAAGGTGCTATT
OCT4	forward	CTTGAATCCCGAATGGAAAGGG
	reverse	GTGTATATCCCAGGGTGATCCTC
c-MYC	forward	AATGAAAAGGCCCCCAAGGTAGTTATCC
	reverse	GTCGTTTCCGCAACAAGTCCTCTTC

3. Results

3.1. Upregulation of RPL27 in CRC:

RPL27 expression was investigated in CRC using the GEPIA database. The level of RPL27 in CRC tissues (n = 275) was higher than that in normal tissues (n = 349) ($p < 0.01$) (Figure 1).

3.2. Silencing of RPL27 inhibits CRC cell growth:

To investigate the effect of RPL27 silencing on cell growth, HCT116 and HT29 cells were transfected with an NCsiRNA or RPL27siRNA. To select the siRNA with the highest transfection efficacy and target gene silencing, three types of RPL27-specific siRNAs (RPL27-1, -2, -3) were tested under optimal transfection conditions. After 96 h, I observed that all the three RPL27siRNAs caused high growth suppression in both HCT116 and HT29 cells, as determined by microscopic observation and MTT assay (Figure 2A&B). The proliferation caused by the three siRNAs was reduced by over 50% compared to that in the control group. Next, I checked the mRNA level of RPL27 after transfection using qRT-PCR (Figure 3A&B). All the three siRNAs significantly inhibited the expression of the RPL27 gene; however, the degree of inhibition caused by RPL27-1siRNA was the highest. In concordance with this short-term observation, transfection of RPL27-1siRNA efficiently blocked long-term colony formation, reducing it by approximately 90% and 86% in HCT116 and HT29 cells, respectively, after seven and nine days of target siRNA transfection (Figure 4A&B).

The ability of RPL27-3siRNA to inhibit colony formation in HCT116 and HT29 cells was similar (Figure 5A&B). As these screening tests identified RPL27-1 as the most potent siRNA, it was used in all subsequent studies. These results suggest that RPL27 is functionally involved in colon tumor cell survival.

3.3. Silencing of RPL27 suppresses cell cycle progression and induces apoptosis:

I then explored whether the inhibition of CRC cell growth via RPL27 knockdown was elicited by a delay in cell cycle progression and/or induction of apoptotic cell death. Flow cytometry analysis confirmed that RPL27 knockdown cells displayed an increased proportion of sub-G_1 phase cells in both HCT116 and HT29 cells (Figure 6A&B). As the sub-G_1 population contains apoptotic cells, the apoptosis assay was examined by staining CRC cells with Annexin V, an apoptotic marker. This showed that targeting RPL27 increased the number of apoptotic cells 72 h after transfection (Figure 7A&B). These results indicate that RPL27 knockdown-mediated inhibition of CRC cell growth was occurred due to delay of cell cycle progression and induction of apoptosis.

3.4. Silencing of RPL27 suppresses CRC growth *in vivo*:

To confirm the suppressive effect of RPL27 silencing on *in vivo*, a tumor formation assay was performed in BALB/c nude mice. HCT116 cells transfected with NCsiRNA or RPL27-1siRNA for 24 h were subcutaneously inoculated into the left and right flanks, respectively. The size of each tumor was measured for 21 days at two- or three-day

intervals. After 14 days, a significant difference in size ($p < 0.05$) was observed between the control and RPL27 knockdown groups (Figure 8A&B). The tumor sizes of the control group were larger than those of the RPL27 knockdown groups. After 21 days, a significant difference ($p < 0.01$) was apparent in size and weight between the control and RPL27 knockdown groups (Figure 9A&B). These results show that, under those experimental conditions, targeting RPL27 significantly reduces the growth of human CRC xenografts *in vivo*.

3.5. Knockdown of RPL27 downregulates PLK1 expression:

To elucidate the molecular mechanisms by which RPL27 silencing could induce the observed phenotypic changes, I performed RNA sequencing and compared the patterns of global gene expression in RPL27-knockdown HCT116 and HT29 cells to those of control cells transfected with NCsiRNA. When at least a 2-fold change was defined, global gene expression analysis revealed that silencing of RPL27 resulted in the up- and down-regulation of 697 RNA transcripts in HCT116 and 3,023 RNA transcripts in HT29 cells (Figure 10A). Overlapping of these two gene sets generated a commonly dysregulated list of 228 genes (69 up- and 159 down-regulated genes), which are considered to be common RPL27 knockdown signatures (Figure 10A&B). Subsequent ingenuity pathway analysis (IPA) showed that 228 mRNA transcripts were functionally enriched in the top five networks. In particular, as shown in Figure 11 (top network 1), the expression level of polo-like kinase 1 (PLK1), which is involved in the cell cycle, was downregulated by RPL27 knockdown. I then validated the decrease of

PLK1 mRNA expression using qRT-PCR (Figure 12). Following RPL27 knockdown, PLK1 mRNA levels were reduced in both HCT116 and HT29 cells. Consistent with the transcriptional profiling of RPL27 knockdown, the protein level of PLK1 was reduced as well under the same conditions (Figure 13). This association was confirmed in the TCGA data. RPL27 mRNA expression was positively correlated with PLK1 expression ($R = 0.255$, $p < 0.001$) in human CRC tissues (Figure 14). Subsequent western blotting confirmed that targeting RPL27 decreases the levels of p-CDC25C (ser198), CDK1, and cyclin B1 in both HCT116 and HT29 cells, which are downstream effectors of PLK1 signaling to exert the transition of G2/M cell cycle phase. These findings suggest that targeting RPL27 induces G2/M arrest in CRC cells.

3.6. Targeting RPL27 inhibits CRC cell migration and invasion:

Several previous studies demonstrated that PLK1 silencing leads to decreased migration and invasion in many cancer cells, including colon cancer cells (25-28). Given the functional significance of PLK1 in cancer cell phenotypes and the observation that PLK1 was repressed under RPL27 knockdown conditions, I investigated whether targeting RPL27 could inhibit the metastatic potential of CRC cells using migration and invasion assays. As results, silencing of RPL27 expression effectively reduced the abilities of migration (Figure 15A&B) and invasion (Figure 16A&B) in both HCT116 and HT29 cell populations. Similar to the inhibitory effects of RPL27-1siRNA, transfection of RPL27-3siRNA also significantly suppressed the migration ability of HCT116 and HT29 cells

(Figure 17A&B). These data imply that targeting RPL27 could be a next therapeutic option for both primary CRC treatment and prevention of metastasis or recurrence.

After performing experiments using silencing, I identified whether RPL27 overexpression could reverse the phenotypic changes. Overexpression experiments were performed in HCT116 cells with the lowest basal level of RPL27 (Figure 18A&B). As expected, a HCT116 transfectant with RPL27-expressing vector (Figure 19A&B) exhibited an increase in its migration ability (Figure 20A&B) when compared to control vector-transfected cells.

3.7. RPL27 knockdown reduces stemness:

It was previously shown that a PLK1 inhibitor killed CD133+ colon cancer stem cells (CSCs) (29); therefore, I investigated whether RPL27 targeting could inhibit stemness in CRC. Before studying CD133+ colon cancer, I confirmed that the mRNA levels of the representative stemness markers CD133, NANOG, CD44, OCT4, and c-MYC were reduced when RPL27 was silenced in HT29 cells. Although the expression levels of stemness markers were also decreased in HCT116 cells, CD44 and c-MYC were not significantly reduced (Figure 21A&B). In line with these results, the HT29 cell line was chosen for subsequent studies. Then, I confirmed that transfection with RPL27-1siRNA effectively suppressed sphere formation in HT29 cells compared to the NCsiRNA transfection (Figure 22). Next, I investigated whether the expression of CD133 was also affected by RPL27 silencing in the CD133+ CRC cell population. The CD133+ CSC population was then sorted from the CD133- population of HT29 cells by FACS using an APC-conjugated

CD133 antibody (Figure 23A). The level of CD133 in the CD133+ CSC portion was significantly higher than that in the CD133- portion (Figure 23B). RPL27 knockdown decreased the levels of CD133 and PLK1 in the CD133+ CSC population (Figure 24A&B). These molecular changes reflected the inhibition of growth and sphere formation in the CD133+ cell population (Figure 25A&B). These data imply that RPL27 is functionally associated with cancer stemness and that RPL27 knockdown could block the migratory and invasive properties of primary CRC by eliminating CSCs in the tumor microenvironment.

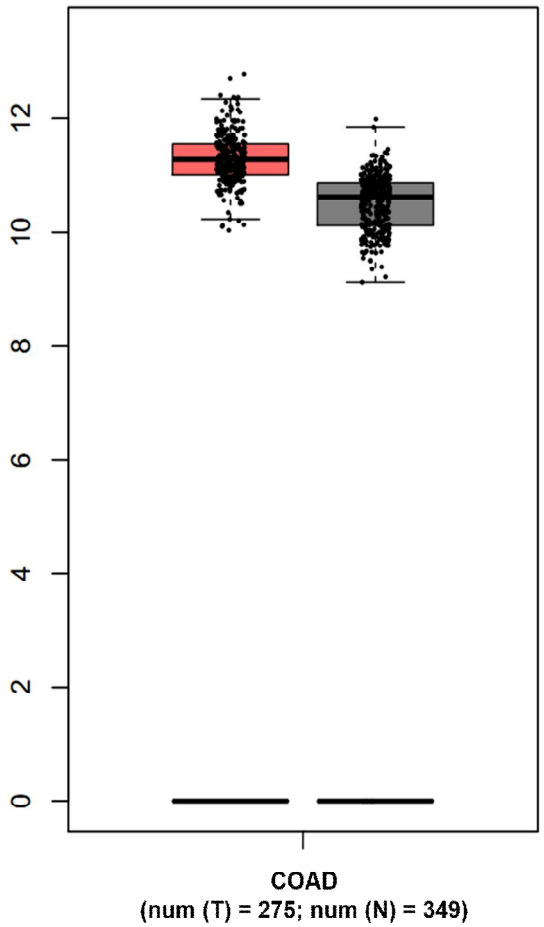

Figure 1. Increased expression of RPL27 in CRC tissues. Red color, tumor tissue (T); gray color, normal tissue (N).

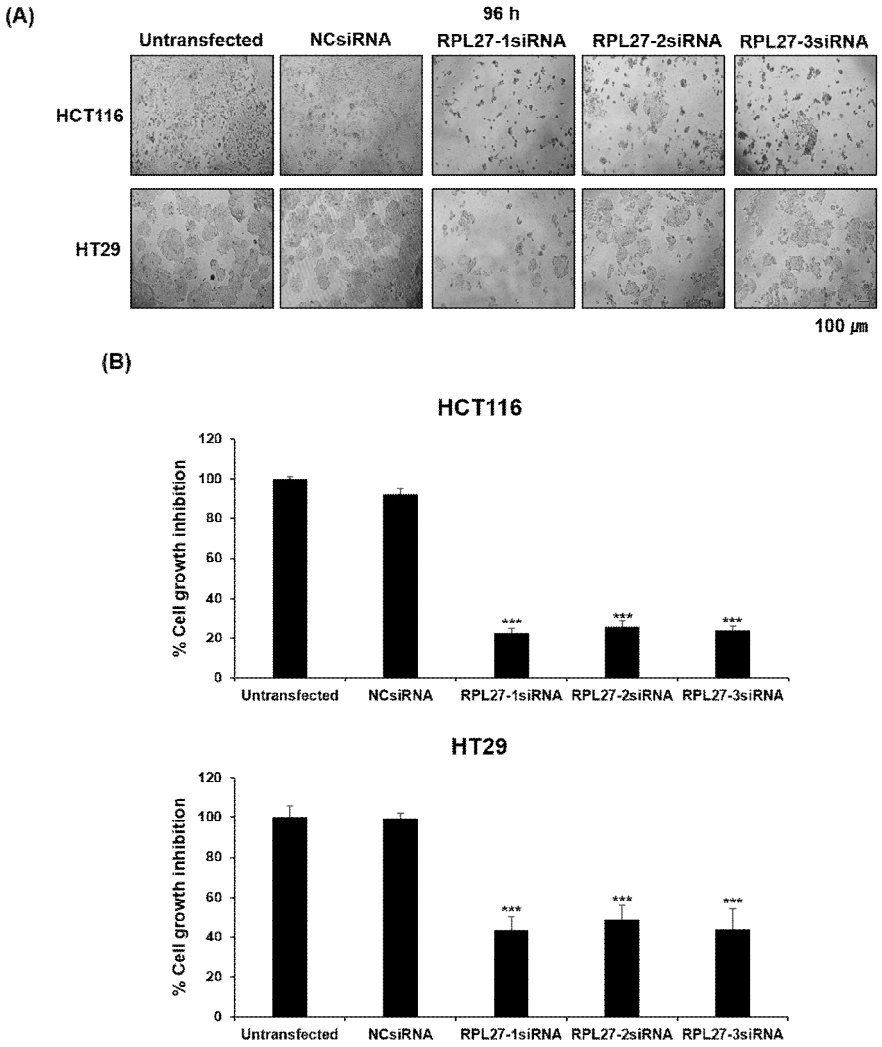

Figure 2. Silencing of RPL27 inhibits CRC cell growth. (A) Light microscopy images of HCT116 and HT29 cells 96 h after transfection with NCsiRNA or three types of RPL27-specific siRNA. Scale bar, 100 ㎛. (B) Growth inhibition of HCT116 and HT29 cells transfected with NCsiRNA or RPL27siRNA for 96 h. NCsiRNA, negative control siRNA; RPL27-1 siRNA, RPL27-2 siRNA, RPL27-3siRNA, three different sequences of RPL27-specific siRNA.

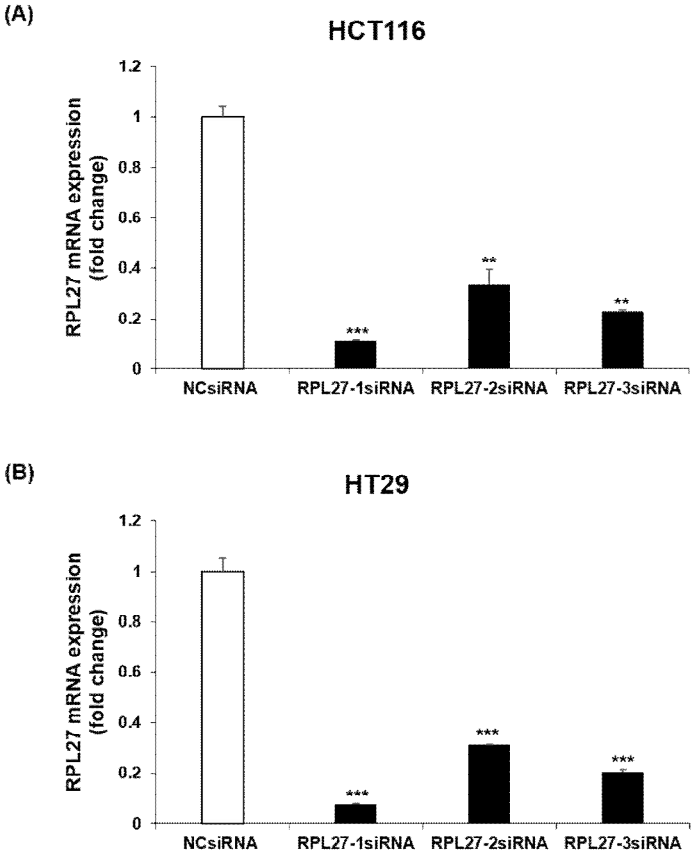

Figure 3. The expression of RPL27 in mRNA level is decreased by RPL27 silencing. (A-B) Detection of RPL27 mRNA expression in HCT116 (A) and HT29 cells (B) at 48 h after transfection. The data are shown relative to GAPDH expression and normalized to NCsiRNA transfection.

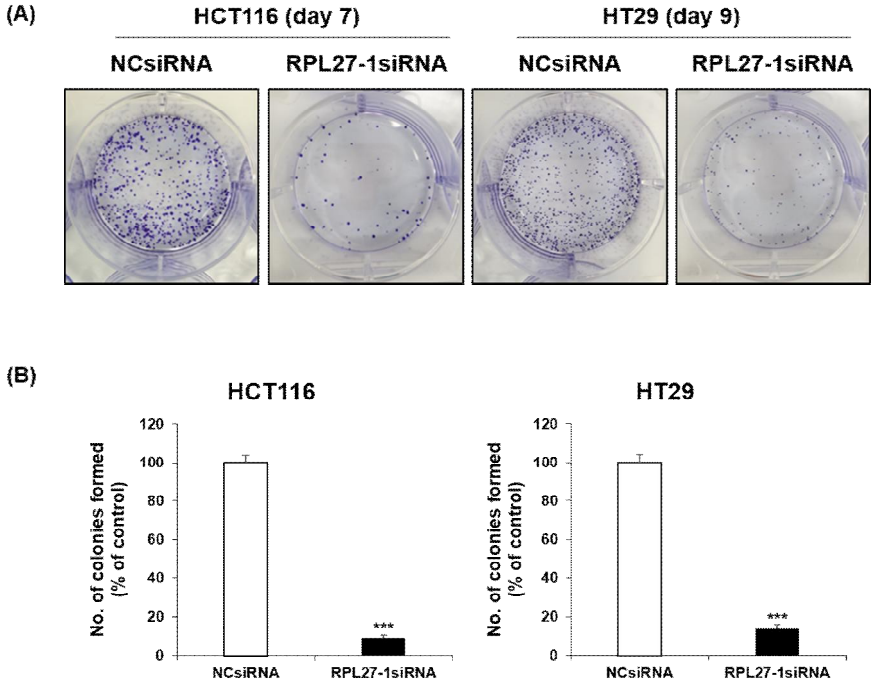

Figure 4. Transfection of RPL27-1siRNA decreases the clonogenicity of CRC cells. (A) Observation of changes in the clonogenicity of HCT116 and HT29 cells after RPL27-1siRNA transfection. (B) The number of colonies was counted in each cell line.

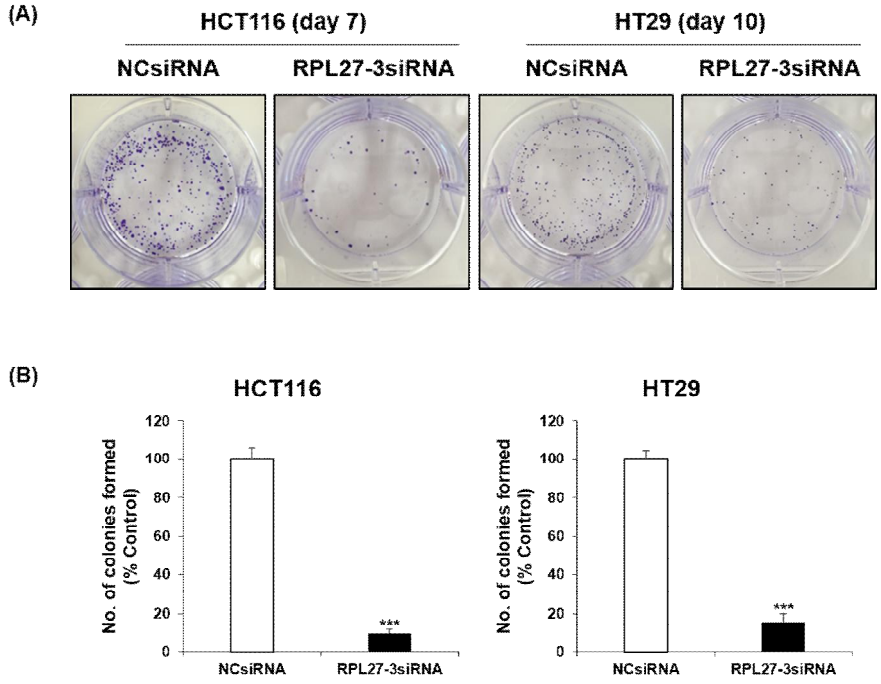

Figure 5. Transfection of RPL27-3siRNA decreases the clonogenicity of CRC cells. (A) Observation of changes in the clonogenicity of HCT116 and HT29 cells after RPL27-3siRNA transfection. (B) The number of colonies was counted in each cell line.

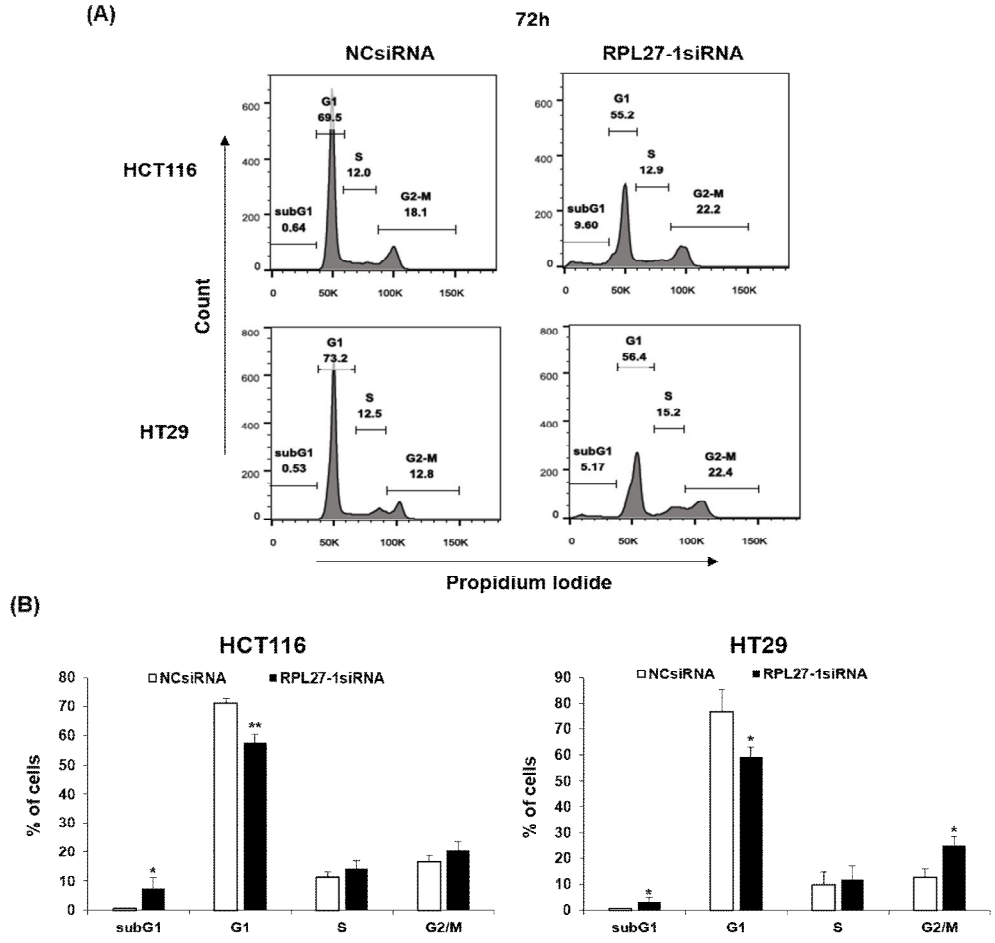

Figure 6. Silencing of RPL27 blocks cell cycle progression. (A) Changes in cell cycle progression were measured by flow cytometry and presented in a histogram at 72 h after siRNA transfection. (B) Percentage of cells in each cell cycle phase is shown as a bar graph.

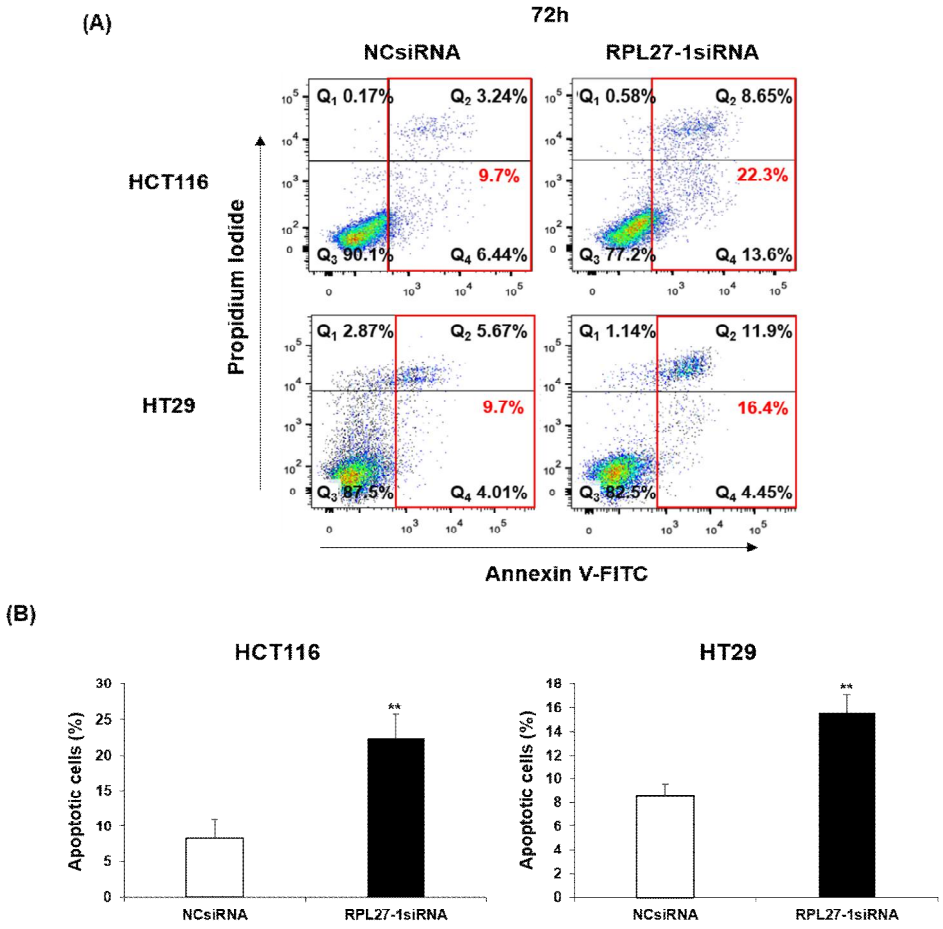

Figure 7. Silencing of RPL27 induces apoptotic cell death. (A) The fraction of apoptotic cells was measured by flow cytometry at 72 h after siRNA transfection. (B) The total percentage of apoptotic cells in the Q2 + Q4 region is shown in a bar graph.

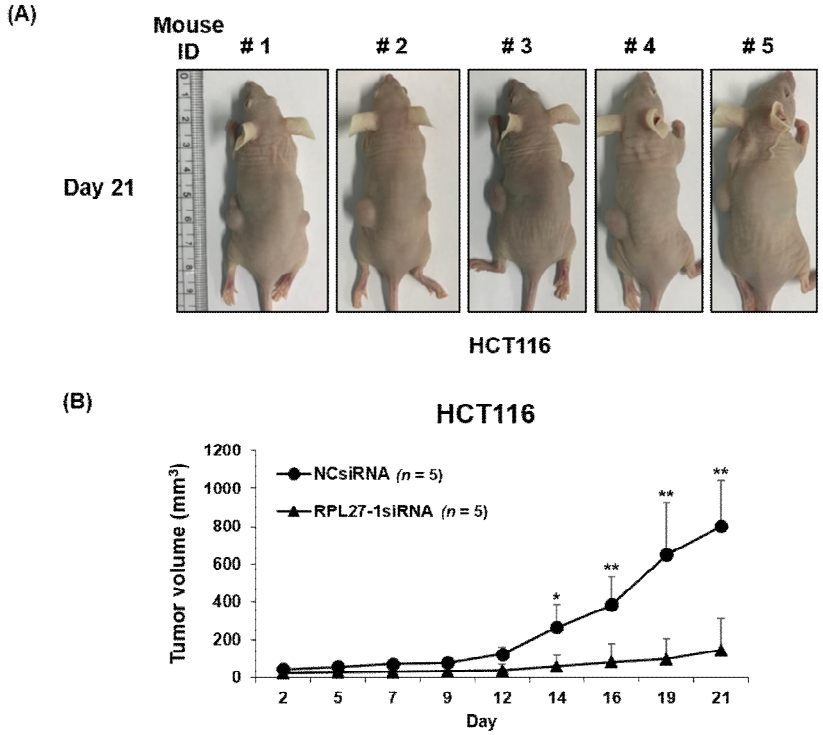

Figure 8. Targeting RPL27 suppresses CRC growth *in vivo*. (A) Observation of differences in tumor sizes between NCsiRNA and RPL27-1siRNA transfected xenografts. (B) Tumor diameters were measured on the indicated days using digital calipers.

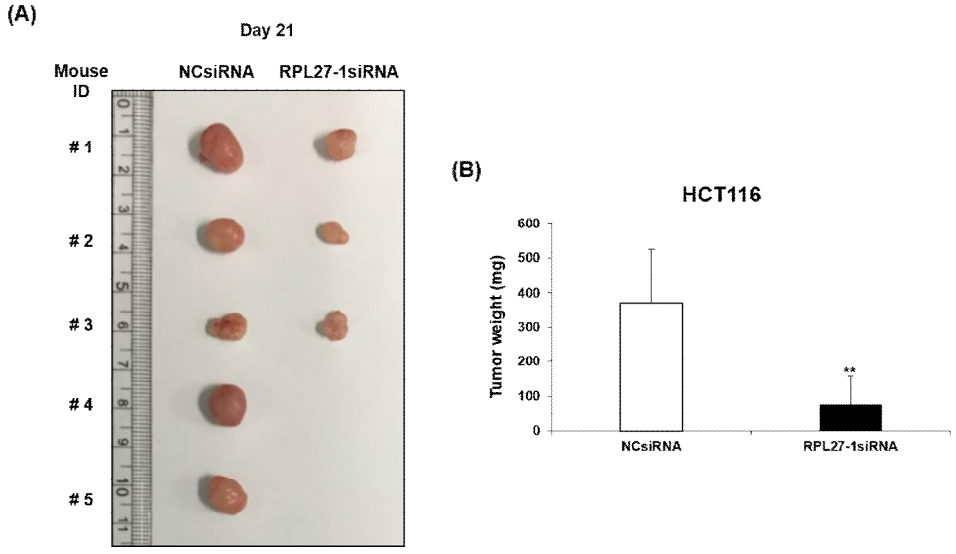

Figure 9. Targeting RPL27 reduces xenograft tumor size. (A) Comparison of the final tumor sizes after transfection with NCsiRNA or RPL27-1siRNA. (B) Measurement of the tumor weight in control and RPL27 knockdown group.

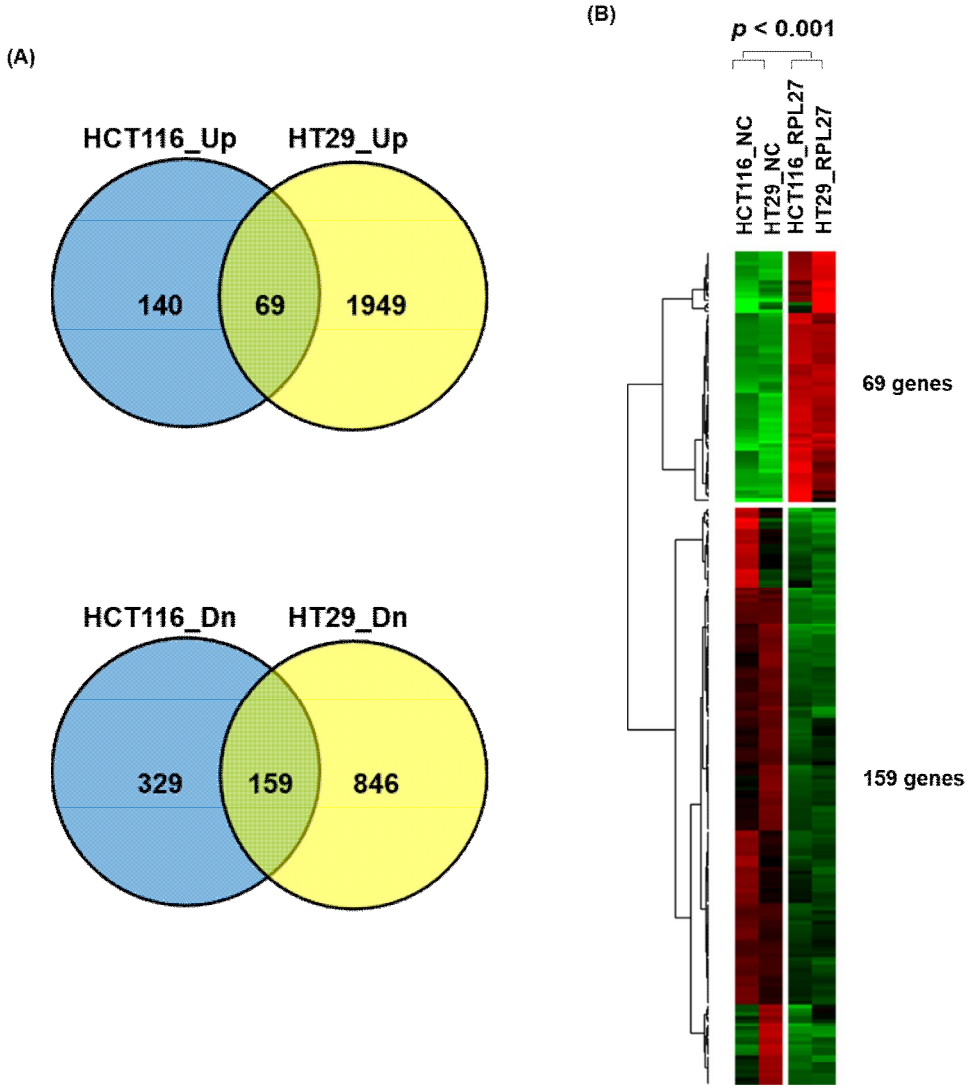

Figure 10. Identification of 228 genes that are commonly up- or down-regulated by RPL27 silencing. (A) The number of genes dysregulated in HCT116 and HT29 cells over 48 h of RPL27-1siRNA transfection. (B) A heat map of the 228 commonly upregulated or downregulated genes in HCT116 and HT29 cells. $p < 0.001$, red (upregulated) and green (downregulated).

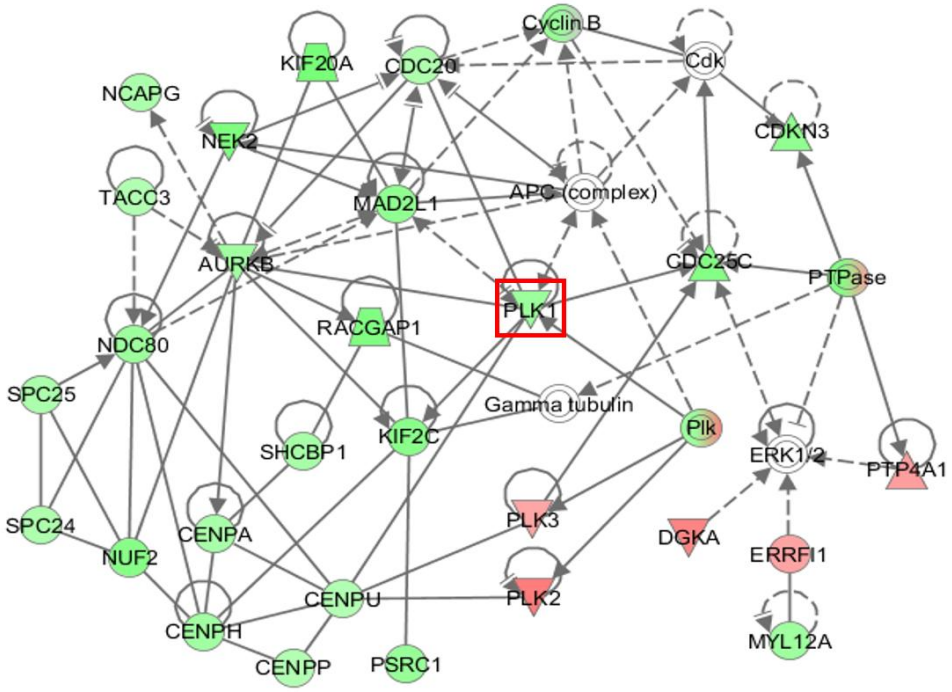

Figure 11. IPA top network 1 functionally associated with PLK1. Up- and down-regulated genes are shown in red and green, respectively. Genes in gray are associated with the regulated genes.

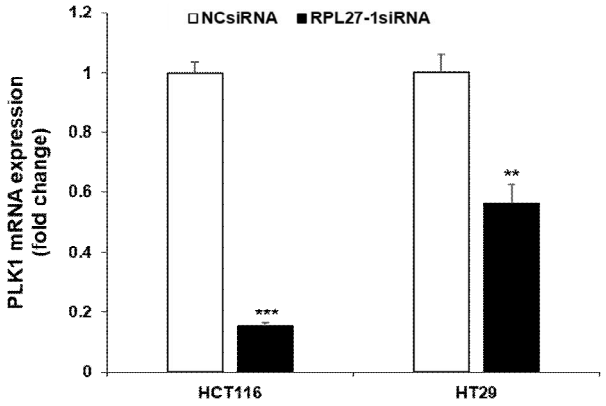

Figure 12. The expression of PLK1 in mRNA level is decreased by RPL27 silencing. Detection of PLK1 mRNA expression 48 h after RPL27-1siRNA transfection of HCT116 and HT29 cells.

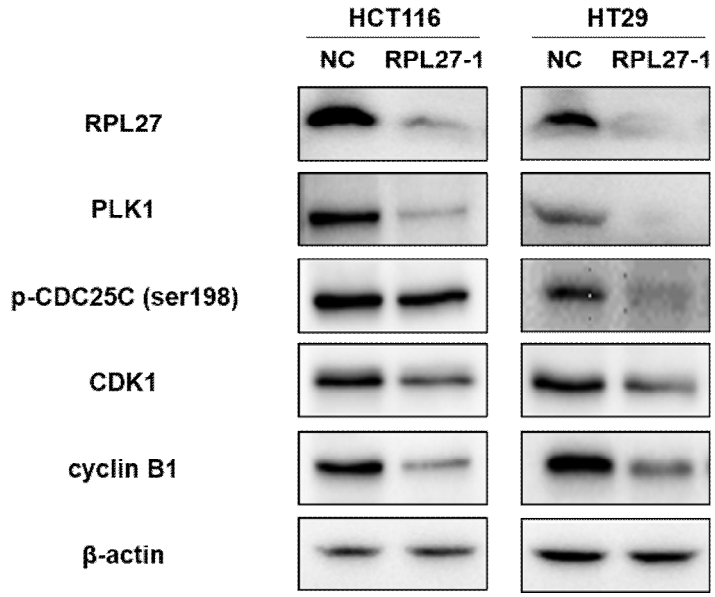

Figure 13. Knockdown of RPL27 disrupts PLK1 signaling. The expression of RPL27, PLK1, p-CDC25C (ser198), CDK1, and cyclin B1 in HCT116 and HT29 cells with RPL27-1siRNA depletion was determined by western blotting. β-actin was used as a loading control.

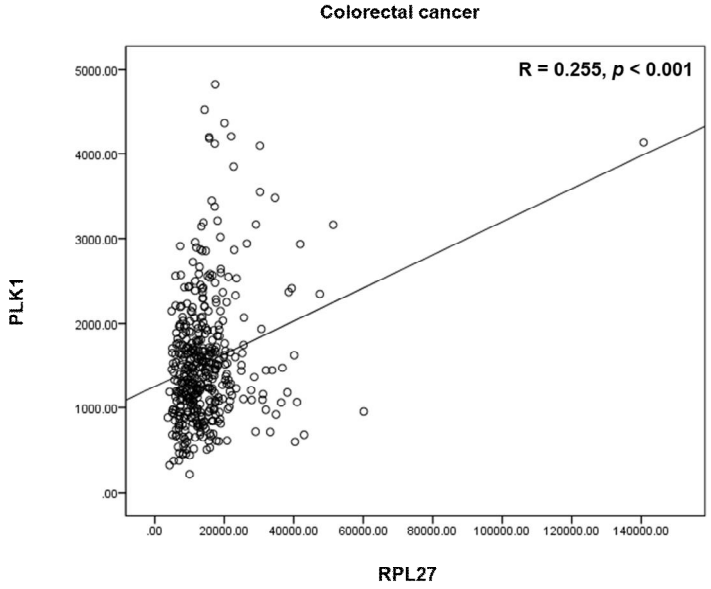

Figure 14. The increased expression of RPL27 is positively correlated with PLK1 expression during CRC development.

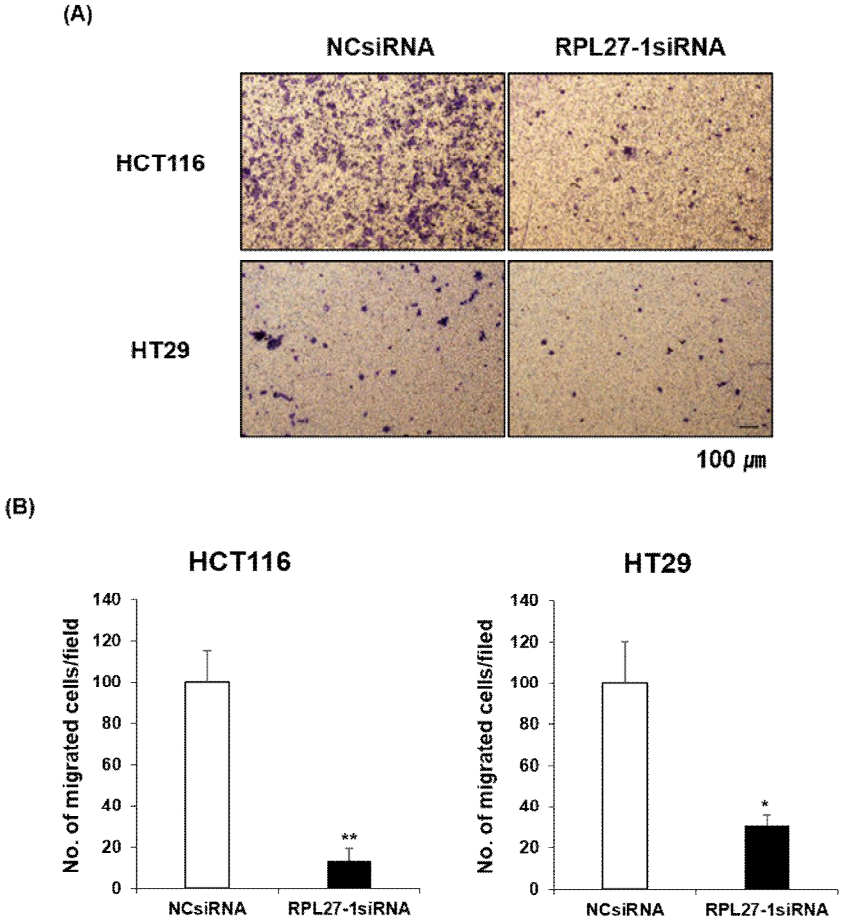

Figure 15. Transfection of RPL27-1siRNA inhibits CRC cell migration. (A) Light microscopy images of migratory NCsiRNA or RPL27-1siRNA transfected HCT116 and HT29 cells. (B) The number of migrated cells was counted and graphed after siRNA transfection.

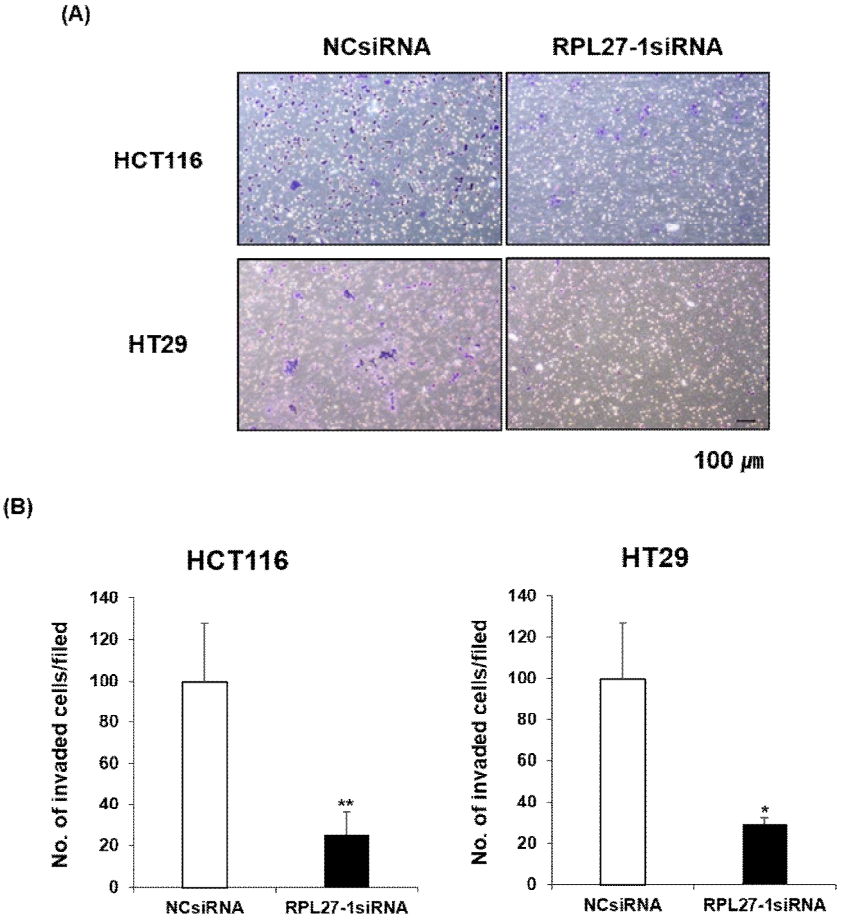

Figure 16. Transfection of RPL27-1siRNA inhibits CRC cell invasion. (A) Light microscopy images of invasive NCsiRNA or RPL27-1siRNA transfected HCT116 and HT29 cells. (B) The number of invaded cells was counted and graphed after siRNA transfection.

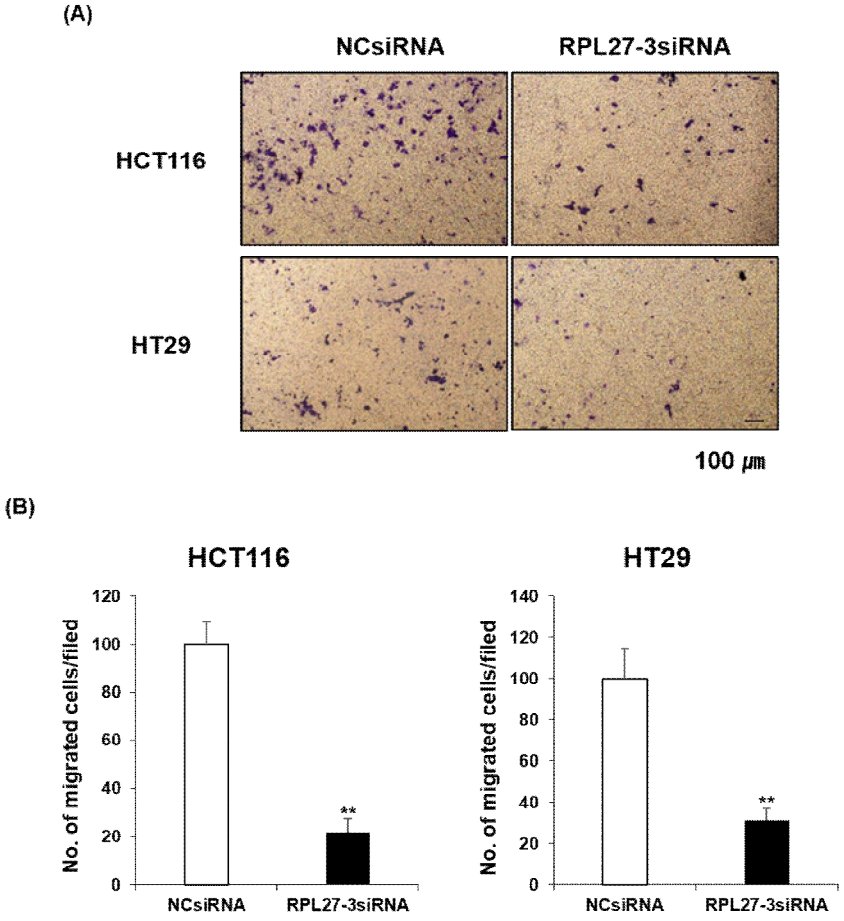

Figure 17. Transfection of RPL27-3siRNA inhibits CRC cell migration. (A) Light microscopy images of migratory NCsiRNA or RPL27-3siRNA transfected HCT116 and HT29 cells. (B) The number of migrated cells was counted and graphed after siRNA transfection.

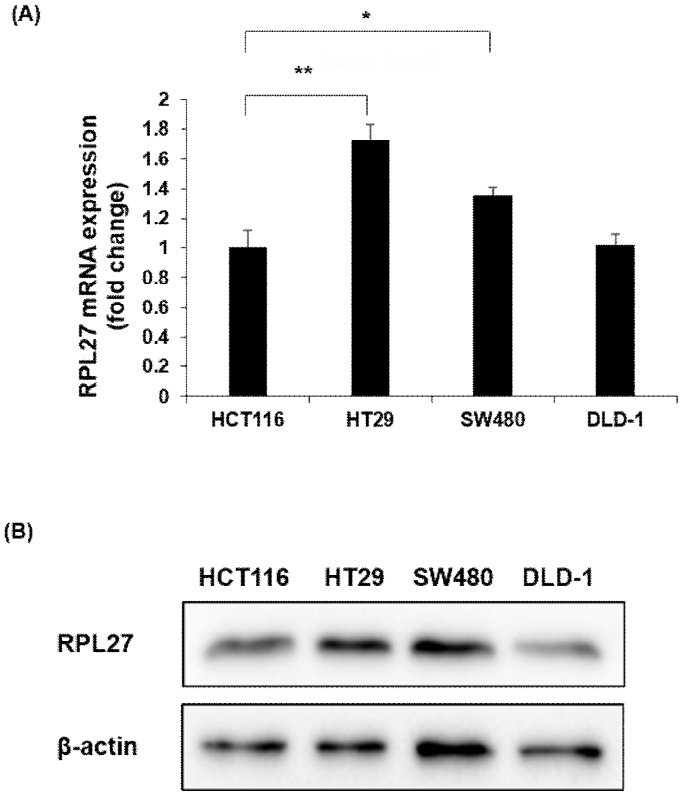

Figure 18. HCT116 cells express RPL27 at the lowest level. Relative basal levels of RPL27 mRNA (A) and protein (B) in HCT116, HT29, SW480, and DLD-1 cells.

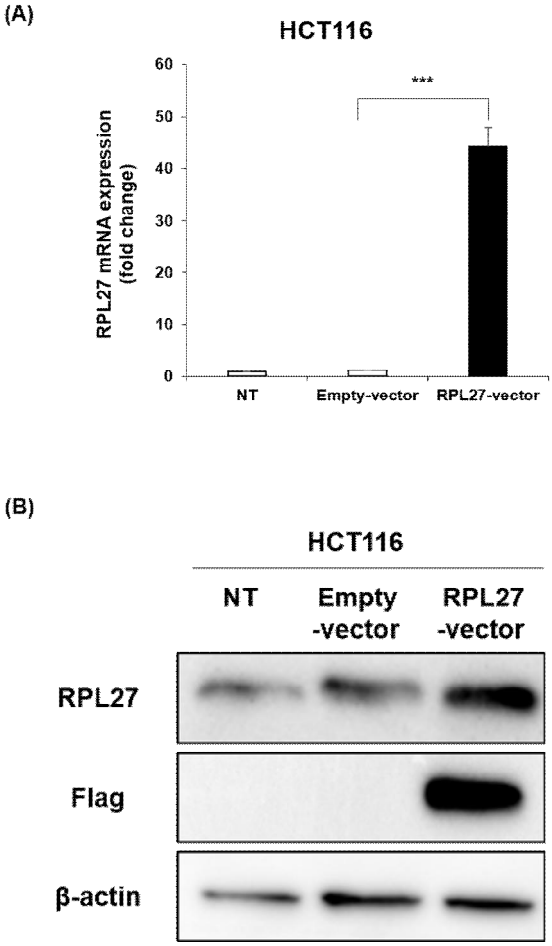

Figure 19. Overexpression of RPL27 in HCT116 cells. Detection of RPL27 mRNA (A) and protein (B) in HCT116 cells that were NT or transfected with an Empty-vector or RPL27-vector. NT, no treatment; Empty vector, transfected with empty control vector; RPL27-vector, transfected with RPL27-expressing vector.

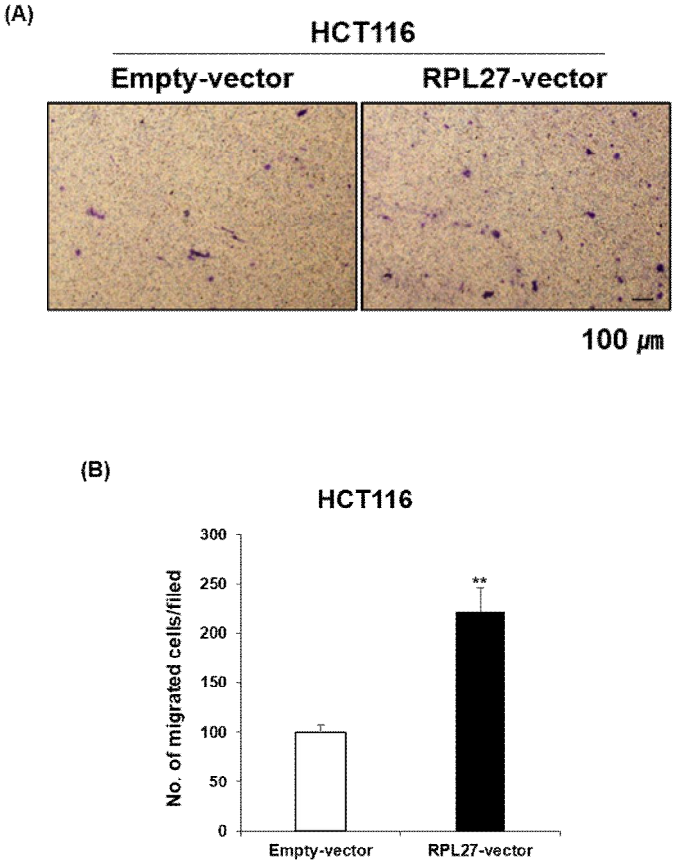

Figure 20. RPL27 promotes the migration of CRC cells. (A) Representative light microscopy images of migratory HCT116 cells transfected with an empty control vector or RPL27-overexpressing vector. (B) The number of migrated cells was counted and graphed.

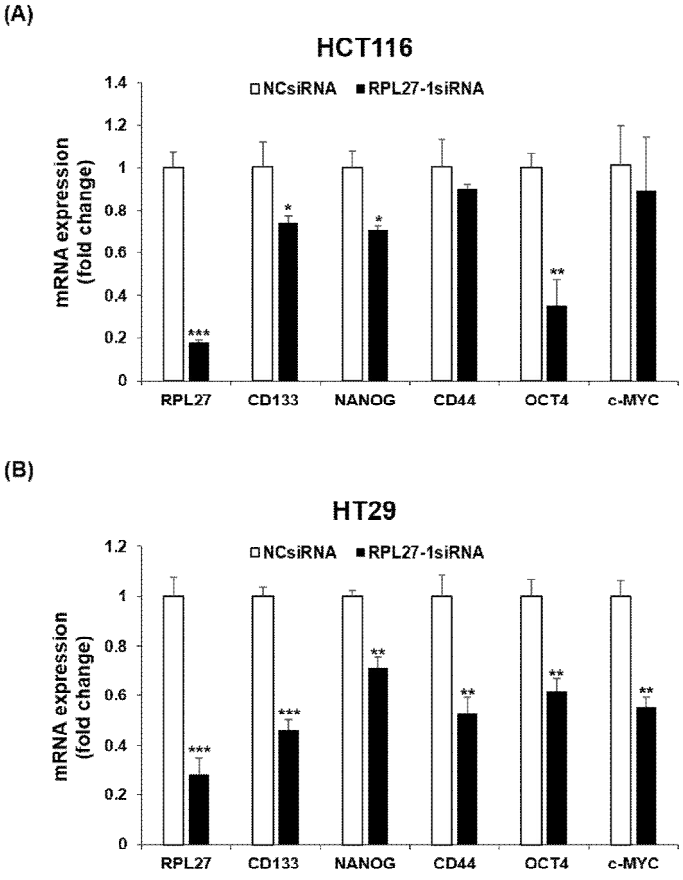

Figure 21. Silencing of RPL27 reduces the expression of cancer stemness genes. Detection of mRNA expression of RPL27 and representative stemness genes in HCT116 (A) and HT29 cells (B) at 48 h after siRNA transfection.

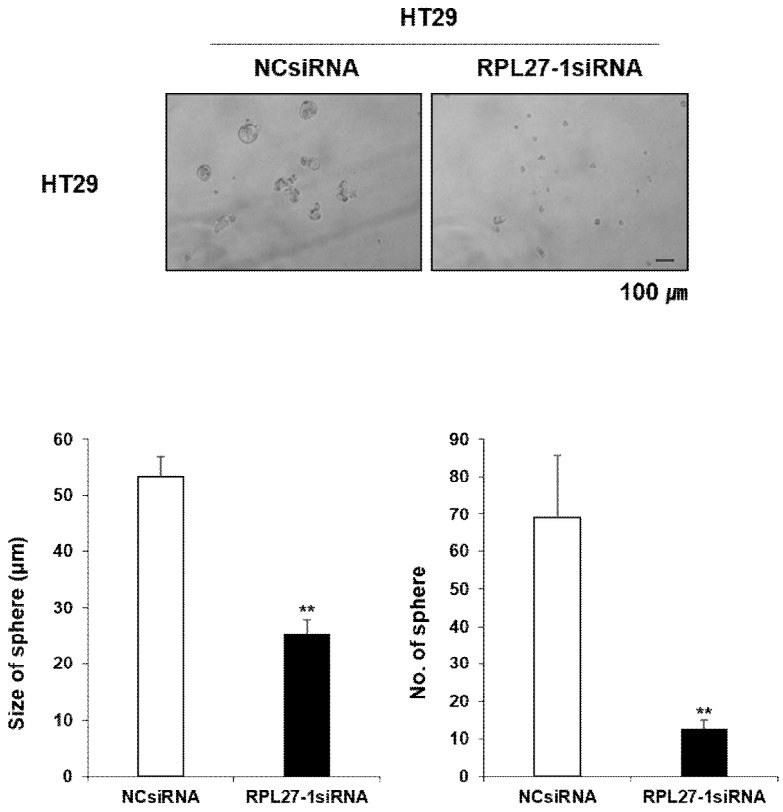

Figure 22. Targeting RPL27 reduces the sphere forming capacity in CRC cells. Detection of sphere formation in HT29 cells after siRNA transfection.

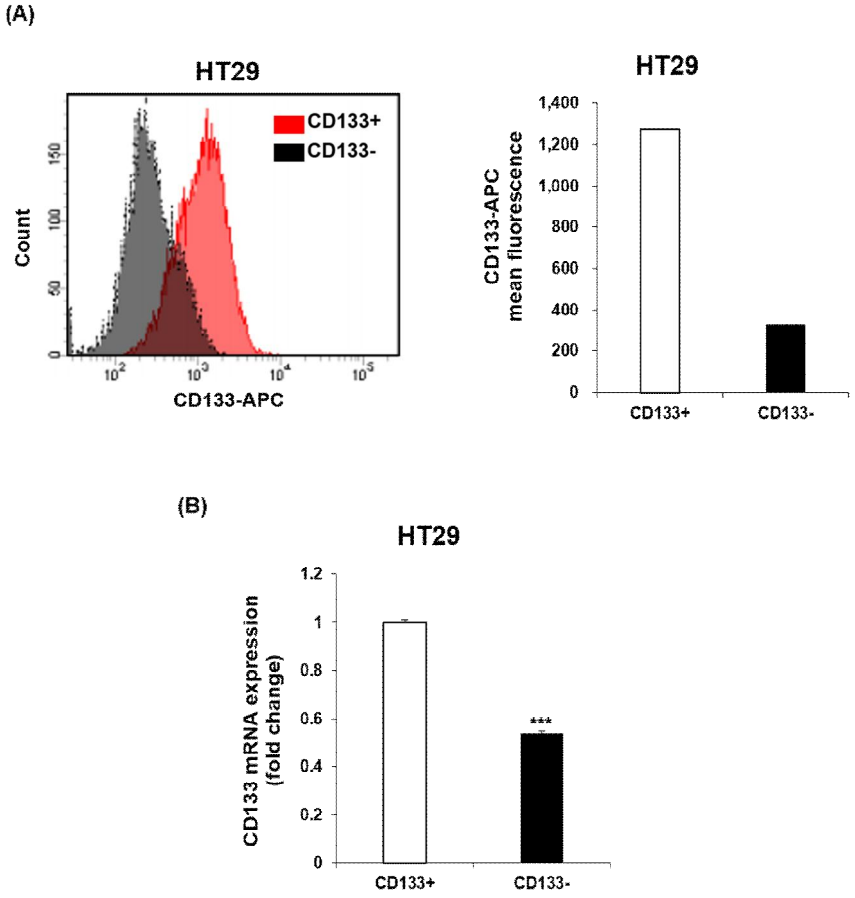

Figure 23. Isolation of CD133+ HT29 cell population from parental cell culture. (A) The results confirmed by FACS after separation of CD133+ CSC population. (B) Relative level of CD133 mRNA in between CD133+ and CD133- cell populations.

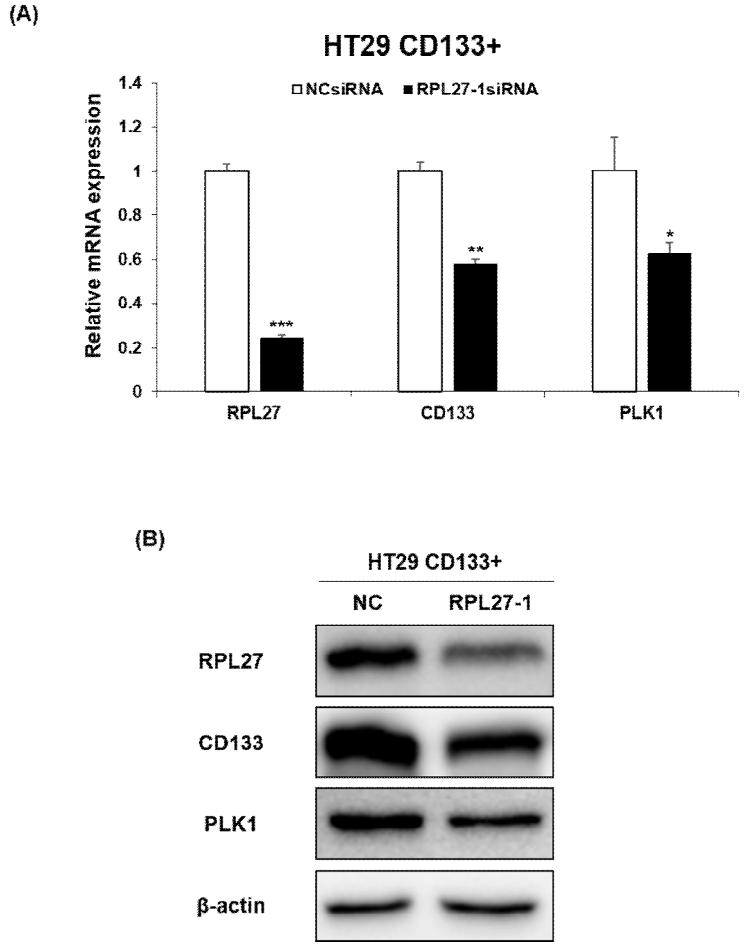

Figure 24. RPL27 knockdown reduces the expression of both CD133 and PLK1 genes in CD133+ HT29 cell population. (A) Changes in mRNA expression of the indicated genes in the CD133+ population transfected with RPL27-1siRNA. (B) Changes in the levels of the indicated proteins in the CD133+ population transfected with RPL27-1siRNA.

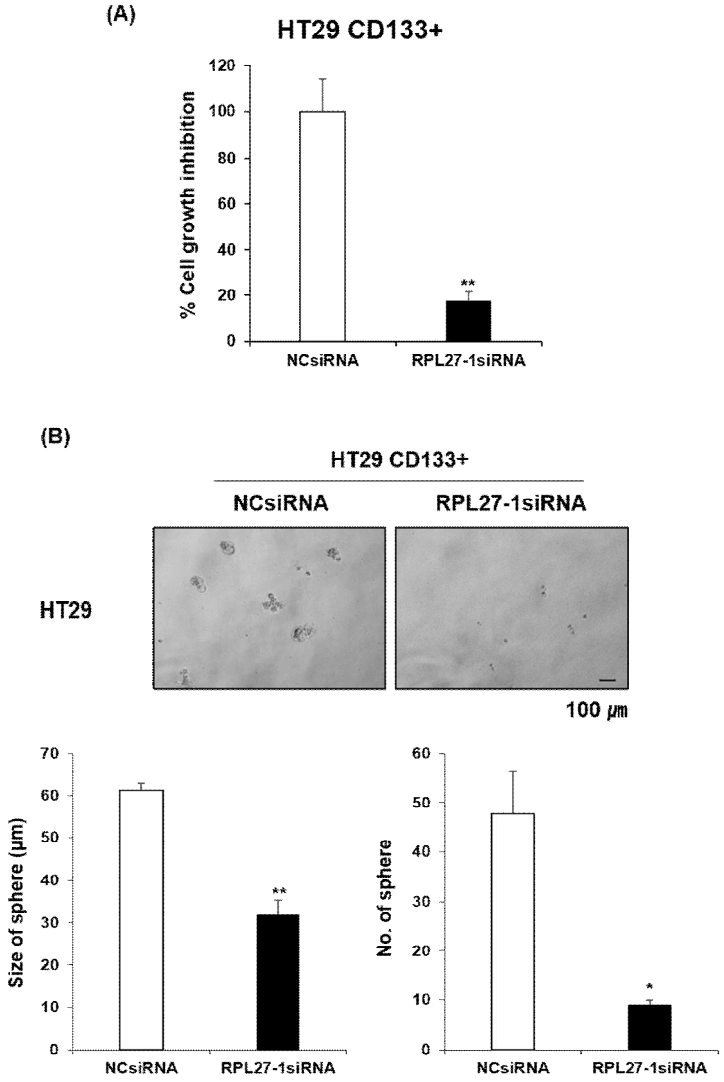

Figure 25. RPL27 knockdown inhibits proliferation and sphere forming capacity of CD133+ HT29 cell population. (A) Inhibition of growth of the CD133+ population transfected with RPL27-1siRNA. (B) Detection of sphere formation of the CD133+ population transfected with RPL27-1siRNA.

4. Discussion

In previous studies, many RPs have been found to be involved in liver cancer cell growth. In addition to RPL27, RPS25, RPS8, and RPS24 are associated with hepatocellular growth (23). Moreover, another study revealed that RPL9, another RP, inhibits the growth of CRC through Id-1/NF-κB signaling (24). Based on the previous studies, RPL27 might affect the growth of CRC.

In network 1 of the IPA analysis, I confirmed that PLK1 was downregulated (Figure 11). PLK1, which is overexpressed in CRC (29,30), is a serine/threonine protein kinase in the polo-like kinase (PLK) family (31). PLK1 is overexpressed in various cancers, including breast cancer (32), renal cancer (33), hepatocellular carcinoma (34), and lung cancer (35). Its functions include mitosis entry and G2/M checkpoint control, centrosome and cell cycle regulation, spindle assembly and chromosome separation regulation, promotion of DNA replication, and cytokinesis and meiosis (36). Previous studies have shown that PLK1 depletion induces apoptosis in various types of cancer cells (37,38). Many studies have shown that PLK1 functions as a target gene for cancer treatment. However, the results of studies on the correlation between RPL27 and PLK1 have not been revealed. Therefore, I determined the extra-ribosomal function of RPL27 in association with PLK1. PLK1 plays several roles in the cell cycle. PLK1 controls the activity of the CDK1/cyclin B1 complex which plays a vital role in the transition of the G2/M phase of the cell cycle by phosphorylating CDC25C (39,40). Western blotting (Figure 13) showed that the protein levels of PLK1, p-CDC25C (ser198), CDK1, and cyclin B1 were decreased in RPL27 knockdown HCT116 and HT29 cells, suggesting cell

cycle arrest in G2/M phase (41,42). In addition, cell cycle analysis performed using FACS showed that the number of G2/M phase cells increased when RPL27 was silenced (Figure 6).

The inhibition of PLK1 led to growth inhibition in colon cancer stem cells, normal pediatric neural stem cells, and breast stem cells (29,43,44). It has been reported that CD133 is regarded as a marker for the isolation and identification of CSC in colon cancer (45). In this study, I observed that RPL27 knockdown blocked cell cycle progression by PLK1 (Figure 13), and that RPL27 depletion decreased the levels of stemness markers (Figures 21&24) and sphere formation (Figures 22&25B) in parental CRC cells and CD133+ fraction. In HCT116 cells, the result could not be observed because spheres were not formed (data not shown). Here, I reported for the first time that the function of RPL27 is correlated with CRC stemness.

In conclusion, this study suggested that RPL27 has extra-ribosomal functions. To my knowledge, this is the first study to show that silencing of RPL27 suppresses proliferation in CRC and stemness. Furthermore, I demonstrated that RPL27 functionally interacts with PLK1 to promote CRC progression. Therefore, RPL27 may be a molecular target for the treatment of CRC.

5. Summary

This study was performed to elucidate the novel function of RPL27 in CRC. When RPL27 was silenced, cell proliferation inhibition and apoptosis induction in HCT116 and HT29 cells were observed. RPL27 silencing also inhibited tumor formation in an *in vivo* experiment using xenograft mice. RNA sequencing revealed that the expression of PLK1 was inhibited by RPL27 knockdown in both cell lines. Subsequent experiments confirmed that RPL27 silencing caused G2/M arrest and decreased migration and invasion abilities. In addition, RPL27 silencing reduced the stemness of CRC. This study demonstrated for the first time that RPL27 may be a potential therapeutic target for CRC.

References

1. Sung H, Ferlay J, Siegel RL, Laversanne M, Soerjomataram I, Jemal A, et al.: Global Cancer Statistics 2020: GLOBOCAN Estimates of Incidence and Mortality Worldwide for 36 Cancers in 185 Countries. CA Cancer J Clin 2021; 71: 209-249.

2. Chan DS, Lau R, Aune D, Vieira R, Greenwood DC, Kampman E, et al.: Red and processed meat and colorectal cancer incidence: meta-analysis of prospective studies. PLoS One 2011; 6: e20456.

3. Fedirko V, Tramacere I, Bagnardi V, Rota M, Scotti L, Islami F, et al.: Alcohol drinking and colorectal cancer risk: an overall and dose-response meta-analysis of published studies. Ann Oncol 2011; 22: 1958-1972.

4. Jo A, Oh H: Incidence of Colon Cancer Related to Cigarette Smoking and Alcohol Consumption in Adults with Metabolic Syndrome: Prospective Cohort Study. J Korean Acad Nurs 2019; 49: 713-723.

5. von Roon AC, Reese G, Teare J, Constantinides V, Darzi AW, Tekkis PP: The risk of cancer in patients with Crohn's disease. Dis Colon Rectum 2007; 50: 839-855.

6. Ma Y, Yang Y, Wang F, Zhang P, Shi C, Zou Y, et al.: Obesity and risk of colorectal cancer: a systematic review of prospective studies. PLoS One 2013; 8: e53916.

7. Jiang Y, Ben Q, Shen H, Lu W, Zhang Y, Zhu J: Diabetes mellitus and incidence and mortality of colorectal cancer: a systematic review and meta-analysis of cohort studies. Eur J Epidemiol 2011; 26: 863-876.

8. Taylor DP, Burt RW, Williams MS, Haug PJ, Cannon-Albright LA: Population-based family history-specific risks for colorectal cancer: a constellation approach. Gastroenterology 2010; 138: 877-885.

9. Fearon ER, Vogelstein B: A genetic model for colorectal tumorigenesis. Cell 1990; 61: 759-767.

10. Bahnassy AA, Zekri AR, Salem SE, Abou-Bakr AA, Sakr MA, Abdel-Samiaa AG, et al.: Differential expression of p53 family proteins in colorectal adenomas and carcinomas: Prognostic and predictive values. Histol Histopathol 2014; 29: 207-216.

11. Kozovska Z, Gabrisova V, Kucerova L: Colon cancer: cancer stem cells markers, drug resistance and treatment. Biomed Pharmacother 2014; 68: 911-916.

12. Braun MS, Seymour MT: Balancing the efficacy and toxicity of chemotherapy in colorectal cancer. Ther Adv Med Oncol 2011; 3: 43-52.

13. Hu CY, Chan W, Delclos GP, Du XL: Adjuvant chemotherapy and risk of gastrointestinal, hematologic, and cardiac toxicities in elderly patients with stage III colon cancer. Am J Clin Oncol 2012; 35: 228-236.

14. Derenzini M, Montanaro L, Trerè D: Ribosome biogenesis and cancer. Acta Histochem 2017; 119: 190-197.

15. Cai Y, Zhang C, Hao L, Chen J, Xie P, Chen Z: Systematic identification of seven ribosomal protein genes in bighead carp and their expression in response to microcystin-LR. J Toxicol Sci 2016; 41: 293-302.

16. Fisher EM, Beer-Romero P, Brown LG, Ridley A, McNeil JA, Lawrence JB, et al.: Homologous ribosomal protein genes on the human X and Y chromosomes: escape from X inactivation and possible implications for Turner syndrome. Cell 1990; 63: 1205-1218.

17. Draptchinskaia N, Gustavsson P, Andersson B, Pettersson M, Willig TN, Dianzani I, et al.: The gene encoding ribosomal protein S19 is mutated in Diamond-Blackfan anaemia. Nat Genet 1999; 21: 169-175.

18. Liu F, Li Y, Yu Y, Fu S, Li P: Cloning of novel tumor metastasis-related genes from the highly metastatic human lung adenocarcinoma cell line Anip973. J Genet Genomics 2007; 34: 189-195.

19. Sim EU, Bong IP, Balraj P, Tan SK, Jamal R, Sagap I, et al.: A preliminary study of differentially expressed genes in Malaysian colorectal carcinoma cases. J Biosci 2006; 17: 19-37.

20. Pogue-Geile K, Geiser JR, Shu M, Miller C, Wool IG, Meisler AI, et al.: Ribosomal protein genes are overexpressed in colorectal cancer: isolation of a cDNA clone encoding the human S3 ribosomal protein.

Mol Cell Biol 1991; 11: 3842-3849.

21. Kondoh N, Schweinfest CW, Henderson KW, Papas TS: Differential expression of S19 ribosomal protein, laminin-binding protein, and human lymphocyte antigen class I messenger RNAs associated with colon carcinoma progression and differentiation. Cancer Res 1992; 52: 791-796.

22. Wang Y, Cheong D, Chan S, Hooi SC: Ribosomal protein L7a gene is up-regulated but not fused to the tyrosine kinase receptor as chimeric trk oncogene in human colorectal carcinoma. Int J Oncol 2000; 16: 757-762.

23. Lee YH, Moon IJ, Hur B, Park JH, Han KH, Uhm SY, et al.: Gene knockdown by large circular antisense for high-throughput functional genomics. Nat Biotechnol 2005; 23: 591-599.

24. Baik IH, Jo GH, Seo D, Ko MJ, Cho CH, Lee MG, et al.: Knockdown of RPL9 expression inhibits colorectal carcinoma growth via the inactivation of Id-1/NF-κB signaling axis. Int J Oncol 2016; 49: 1953-1962.

25. Han DP, Zhu QL, Cui JT, Wang PX, Qu S, et al.: Polo-like kinase 1 is overexpressed in colorectal cancer and participates in the migration and invasion of colorectal cancer cells. Med Sci Monit 2012; 18: BR237-BR246.

26. Zhang Z, Zhang G, Gao Z, Li S, Li Z, Bi J, et al.: Comprehensive analysis of differentially expressed genes associated with PLK1 in

bladder cancer. BMC Cancer 2017; 17: 861.

27. Song R, Hou G, Yang J, Yuan J, Wang C, Chai T, et al.: Effects of PLK1 on proliferation, invasion and metastasis of gastric cancer cells through epithelial-mesenchymal transition. Oncol Lett 2018; 16: 5739-5744.

28. Wu ZY, Wei N: Knockdown of PLK1 inhibits invasion and promotes apoptosis in glioma cells through regulating autophagy. Eur Rev Med Pharmacol Sci 2018; 22: 2723-2733.

29. Francescangeli F, Patrizii M, Signore M, Federici G, Di Franco S, Pagliuca A, et al.: Proliferation state and polo-like kinase1 dependence of tumorigenic colon cancer cells. Stem cells 2012; 30: 1819-1830.

30. Takahashi T, Sano B, Nagata T, Kato H, Sugiyama Y, Kunieda K, et al.: Polo-like kinase 1 (PLK1) is overexpressed in primary colorectal cancers. Cancer Sci 2003; 94: 148-152.

31. Golsteyn RM, Lane HA, Mundt KE, Arnaud L, Nigg EA: The family of polo-like kinases. Prog Cell Cycle Res 1996; 2: 107-114.

32. Maire V, Némati F, Richardson M, Vincent-Salomon A, Tesson B, Rigaill G, et al.: Polo-like kinase 1: a potential therapeutic option in combination with conventional chemotherapy for the management of patients with triple-negative breast cancer. Cancer Res 2013; 73: 813-823.

33. Zhang G, Zhang Z, Liu Z: Polo-like kinase 1 is overexpressed in renal cancer and participates in the proliferation and invasion of renal cancer cells. Tumour Biol 2013; 34: 1887-1894.

34. He ZL, Zheng H, Lin H, Miao XY, Zhong DW: Overexpression of polo-like kinase1 predicts a poor prognosis in hepatocellular carcinoma patients. World J Gastroenterol 2009; 15: 4177-4182.

35. Yoon HE, Kim SA, Choi HS, Ahn MY, Yoon JH, Ahn SG: Inhibition of Plk1 and Pin1 by 5′-nitro-indirubinoxime suppresses human lung cancer cells. Cancer Lett 2012; 316: 97-104.

36. van de Weerdt BC, Medema RH: Polo-like kinases: a team in control of the division. Cell Cycle 2006; 5: 853-864.

37. Liu X, Erikson RL: Polo-like kinase (Plk)1 depletion induces apoptosis in cancer cells. Proc Natl Acad Sci U S A 2003; 100: 5789-5794.

38. Spänkuch B, Kurunci-Csacsko E, Kaufmann M, Strebhardt K: Rational combinations of siRNAs targeting Plk1 with breast cancer drugs. Oncogene 2007; 26: 5793-5807.

39. Gavet O, Pines J: Activation of cyclin B1-Cdk1 synchronizes events in the nucleus and the cytoplasm at mitosis. J Cell Biol 2010; 189: 247-259.

40. Gutteridge RE, Ndiaye MA, Liu X, Ahmad N: Plk1 Inhibitors in

Cancer Therapy: From Laboratory to Clinics. Mol Cancer Ther 2016; 15: 1427-1435.

41. Hsiao YC, Hsieh YS, Kuo WH, Chiou HL, Yang SF, Chiang WL, et al.: The tumor-growth inhibitory activity of flavanone and 2′-OH flavanone in vitro and in vivo through induction of cell cycle arrest and suppression of cyclins and CDKs. J Biomed Sci 2007; 14: 107-119.

42. Bhosale PB, Vetrivel P, Ha SE, Kim HH, Heo JD, Won CK, et al.: Iridin Induces G2/M Phase Cell Cycle Arrest and Extrinsic Apoptotic Cell Death through PI3K/AKT Signaling Pathway in AGS Gastric Cancer Cells. Molecules 2021; 26: 2802.

43. Kamijo T: Role of stemness-related molecules in neuroblastoma. Pediatr Res 2012; 71: 511-515.

44. Hu K, Law JH, Fotovati A, Dunn SE: Small interfering RNA library screen identified polo-like kinase-1 (PLK1) as a potential therapeutic target for breast cancer that uniquely eliminates tumor-initiating cells. Breast Cancer Res 2012; 14: R22.

45. Zhang H, Li W, Nan F, Ren F, Wang H, Xu Y, et al.: MicroRNA expression profile of colon cancer stem-like cells in HT29 adenocarcinoma cell line. Biochem Biophys Res Commun 2011; 404: 273-278.

Studies on Definition of Novel Functional Roles of RPL27 Gene in Colorectal Cancer Progression

Park, So-Young

Department of Molecular Medicine
Graduate School

Keimyung University

(Supervised by Professor Lee, Yun-Han)

(Abstract)

Ribosomal proteins (RPs) participate in ribosome synthesis and are also associated with cancer. Ribosomal protein L27 (RPL27), one of the RPs, is overexpressed in colorectal cancer (CRC), but its function is still unknown. I have found in this study that inhibition of RPL27 expression by siRNA inhibits CRC cell growth and long-term colony formation through an increase in sub-G_1 phase population and induction of apoptotic cell death. Targeting RPL27 also inhibited the growth of human CRC xenografts in nude mice. RNA sequencing revealed that polo-like kinase 1 (PLK1), which functions in the cell cycle and stemness, was commonly downregulated in HCT116 and HT29 cells. Western blot analysis confirmed that RPL27 silencing decreases the levels of PLK1 and G2/M-associated genes. Importantly, it was further

demonstrated that RPL27 knockdown decreases the levels of CD133 and PLK1 in the CD133+ CSC population. These molecular changes led to the inhibition of cell growth and sphere formation in the CD133+ cell population. Taken together, these findings indicate that silencing of RPL27 suppresses CRC cell growth and stemness via disruption of PLK1 signaling and that targeting RPL27 could be a next-line therapeutic strategy for both primary CRC treatment and prevention of metastasis and/or recurrence.

대장암 발병에 있어 RPL27 유전자의 신규 기능 규명 연구

박 소 영
계명대학교 대학원
의학과 분자의학 전공
(지도교수 이 윤 한)

(초록)

리보솜 합성에 기능하는 리보솜 단백질(RPs)는 암과도 관련이 있다. RPs의 하나인 리보솜 단백질 L27(RPL27)은 인간 대장암에서 과발현하지만, 아직 대장암 발생 과정에서 RPL27의 기능은 잘 알려져 있지 않다. 이에 본 연구에서는, siRNA 기법을 이용하여 RPL27을 표적하였을 때 대장암의 진행과정에 영향을 끼치는지를 우선 조사하였다. 그 결과 RPL27 유전자의 발현 저해가 대조군 처리에 비하여, 대장암 세포주 HCT116 및 HT29의 성장을 억제하며 장기간의 군체 형성 능력도 감소시킴을 확인하였다. 세포사멸 유도 측면에서는, sub-G_1 세포군의 비율이 증가하였고, 세포사멸 유도를 관찰하였다. 또한, RPL27 발현 억제는 누드마우스에 이종 이식한 인간 대장암의 성장을 저해하였다. RNA 염기서열분석 결과, 228개의 유전자가 같은 방향조절을 보였다. 특히, 세포주기와 줄기능 등에 관여하는 것으로 알려진 PLK1 발현이 HCT116과 HT29 세포에서 공통적으로 하향조절됨을 관찰하

였다. 그 다음 웨스턴 블롯 분석을 통해 RPL27 침묵으로 두 세포 모두에서 PLK1과 G2/M관련 유전자들의 수준을 조절하지 못한다는 것을 확인하였고, 이 결과는 G2/M 정지가 일어났음을 의미한다. 추가적으로, TCGA 빅 데이터를 이용하여 대장암 조직에서 RPL27과 PLK1의 mRNA 발현이 양의 상관관계가 있음을 확인하였다. 이러한 분자 반응을 반영하여, RPL27 발현 저해가 대장암 세포의 침윤능과 이동능을 감소시켰다. 앞선 결과와 반대로, RPL27을 과발현하였을 때는 이동능이 증가하였다. 다음으로, HT29 세포에서 RPL27 침묵이 줄기세포 마커들의 mRNA 수준이 감소시켰다. 또한, RPL27이 침묵된 HT29 세포에서 구체 형성 능력이 감소되었다. 중요하게, CD133+ 세포 집단에서 RPL27 침묵에 의해 CD133과 PLK1의 발현 수준이 감소함을 확인하였다. 이러한 분자 변화는 CD133+ 세포 집단에서 세포 성장 및 구체 형성의 억제를 일으켰다. 이러한 발견은 RPL27을 표적하는 것이 대장암 성장을 억제하고 G2/M 정지를 통해 대장암 줄기능을 감소시킨다는 것을 나타낸다. RPL27 표적은 1차 대장암의 성장 억제뿐만 아니라 전이 및 재발도 동시에 억제할 수 있는 차세대 치료 전략이 될 수 있다.

□ 저자 약력

1994년 대구 출생
영남대학교 생명공학부 분자생명과학전공 졸업
계명대학교 대학원 의학과 석사

□ 논문 및 저서

「Targeting CALM2 Inhibits Hepatocellular Carcinoma Growth and Metastasis by Suppressing E2F5-mediated Cell Cycle Progression」 Anticancer Research 2021. 3.
「Silencing CDCA8 Suppresses Hepatocellular Carcinoma Growth and Stemness via Restoration of ATF3 Tumor Suppressor and Inactivation of AKT/β-Catenin Signaling」 Cancers 2021. 3.